J. Am. Soc. Mass Spectrom. (2012) 23:858–868
DOI: 10.1007/s13361-012-0343-9

RESEARCH ARTICLE

# Revisiting the Reactivity of Uracil During Collision Induced Dissociation: Tautomerism and Charge-Directed Processes

Daniel G. Beach, Wojciech Gabryelski

Department of Chemistry, University of Guelph, Guelph, Ontario, N1G 2W1, Canada

**Abstract**

In our recent work towards the nontarget identification of products of nucleic acid (NA) damage in urine, we have found previous work describing the dissociation of NA bases not adequate to fully explain their observed reactivity. Here we revisit the gas-phase chemistry of protonated uracil (U) during collision induced dissociation (CID) using two modern tandem mass spectrometry techniques; quadrupole ion trap (QIT) and quadrupole time of flight (Q-TOF). We present detailed mechanistic proposals that account for all observed products of our experiments and from previous isotope labeling data, and that are supported by previous ion spectroscopy results and theoretical work. The diverse product-ions of U cannot be explained adequately by only considering the lowest energy form of protonated U as a precursor. The tautomers adopted by U during collisional excitation make it possible to relate the complex reactivity observed to reasonable mechanistic proposals and feasible product-ion structures for this small highly conjugated heterocycle. These reactions proceed from four different stable tautomers, which are excited to a specific activated precursor from which dissociation can occur via a charge-directed process through a favorable transition state to give a stabilized product. Understanding the chemistry of uracil at this level will facilitate the identification of new modified uracil derivatives in biological samples based solely on their reactivity during CID. Our integrated approach to describing ion dissociation is widely applicable to other NA bases and similar classes of biomolecules.

**Key words:** DNA damage, FAIMS, High-field asymmetric waveform ion mobility spectrometry, Differential mobility spectrometry, DMS, RNA, Nontarget identification, Metabolomics

## Introduction

Our recent work has been directed towards the nontarget identification of urinary biomarkers of nucleic acid damage and metabolism [1]. These compounds, which are detected as modified nucleosides or bases in urine, can provide important information about DNA [2] or RNA damage [3] that has occurred in the cell. The identification of low abundance unknown species such as these in a complex biological sample matrix remains a significant challenge for any analytical technique. High resolution tandem mass spectrometry (MS/MS) with a suitable analytical separation has a realistic possibility of addressing this challenge, and we have recently shown some success in this direction [1, 4, 5]. However, in addition to the instrumental challenges associated with acquiring high quality spectra for metabolites in urine [1], the interpretation of MS/MS data for the purpose of unknown identification remains a significant challenge. Such de novo identification aims to correlate observed spectral features in MS/MS to the structures of investigated species based on established reactivity for a class of compounds [4, 6–9]. The idea of using MS/MS as stand-alone identification tool is of increasing interest and is also being addressed using other more general approaches intended to generalize dissociation pathways [10], to automate data analysis [11], or to compile spectra in databases [12, 13].

*Correspondence to:* Wojciech Gabryelski; *e-mail:* wgabryel@uoguelph.ca

Received: 24 October 2011
Revised: 13 January 2012
Accepted: 17 January 2012
Published online: 14 February 2012

All nucleosides and NA bases as well as a large number of their isotopically labeled analogues and modified species have been studied by CID [14–18]. These reports have allowed for the facile and selective detection of those target analytes in biological samples as well as some other compounds that showed similar fragmentation patterns. Knowing a compound's fragmentation pattern allows one to recognize modified species when they show analogous dissociation patterns. Understanding a compound's gas-phase ion chemistry on a mechanistic level is a much more powerful tool in de novo identification. This understanding allows both analogous and unique fragmentation patterns of derivatives to be correlated to their chemical structures, which can be explained in terms of actual chemical reactions. For example, the identification of pyrimidine ring methylated guanosines in biological samples is relatively routine [19–21]. This is because these ions exhibit pyrimidine ring fragmentation pathways matching those of guanine, whose mechanisms were fully described [14]. However, even minor modifications of nucleobases can drastically alter their fragmentation patterns. The best example is hydroxylation of 2'-deoxyguanosine at the C-8 position to produce 8-oxo-2'-deoxygaunosine. This modification not only completely suppresses the elimination of the deoxyribose moiety [22], which is used for recognizing deoxynucleoside ions, but it also changes the mechanism of pyrimidine ring decomposition. It can easily be envisioned that without prior knowledge, identification of this DNA oxidation product and its derivatives in a real sample might not be trivial. It is, therefore, important to understand and interpret data from tandem mass spectrometry in terms of the actual chemical reactions occurring in the gas-phase so that spectral features can better be correlated to the structure of unknown species.

The dissociations of conjugated heterocycles including NA bases is known to be particularly complex, and their mechanisms are of fundamental interest. Ions with a fixed charge site or little conjugation can undergo charge-remote dissociation that is similar in mechanism to thermal degradation of neutral molecules [23, 24]. In contrast, the small, highly conjugated ions of NA bases typically react through charge-mediated processes [1, 4, 6, 7, 18, 24]. Intramolecular chemical reactions of precursor ions are initiated by a charge site, and the stability of specific conformations of precursor ions and product-ions are determined by inductive effects, steric effects, and resonance in the conjugated system of double bonds. These chemical effects and their influence on reactivity of the ions of NA bases and their derivatives can be understood, predicted, modeled, and used for the structural elucidation of unknown compounds. A key factor in the gas-phase ion chemistry of NA bases and their derivatives is their tautomerism. Interconversion between the lowest energy tautomer and higher energy tautomeric forms occurs during collisional activation. This adds to the complexity of the gas-phase chemistry of this class of compounds because multiple dissociation pathways involve different tautomeric forms of precursor and product-ions. However, the link between proposed or observed tautomers and detected product-ions has rarely been made [18].

While a great deal of work has previously been done in this field, we have found that there are major gaps in knowledge and the lack of a unified simple model that would be able to explain the reactivity of highly conjugated positive and negative ions of NA bases. We have re-examined the gas-phase ion chemistry of several NA bases and established a suitable model that can explain all their MS/MS spectral features in terms of specific chemical reactions and accounts for changes in reactivity observed in modified analogs. Interpretation of the reactivity of radical cations in electron ionization (EI) has been developed to the point where spectral interpretation based on simple reaction mechanism is now sophomore lecture material [25]. A better fundamental understanding of CID mechanisms is the first step towards this type of interpretation of MS/MS data in the future.

Based on the hundreds of reaction mechanisms we have examined in our previously published [1, 4–7, 18] and unpublished studies and the fundamental basics of ion dissociation [24, 25], we have developed a unique approach for describing MS/MS reactions of small conjugate ions during CID. In general: (1) Reaction steps can be described as charge-directed processes [24]. (2) Collisionally excited ions can adopt higher energy conformations that are the precursors to dissociation [18, 24, 26]. (3) The activated precursor offers stabilization to the charge as it is developing during the dissociation step. (4) The product of dissociation is stabilized by delocalization of the charge as much as possible given the structure and formula of the ion [25]. (5) Ions with a localized charge are transient species prone to rapid fragmentation and are often not detected in MS/MS spectra. (6) Bond making (nucleophilic attack) or non-dissociative bond breaking (ring opening) occur prior to elimination of a neutral, which is the final step of dissociation forming a stable product.

In this paper, we revisit the gas-phase ion chemistry of protonated U. Uracil and several of its isotopologues has been previously analyzed by fast atom bombardment ionization with low energy CID [16]. However, the reactivity of this fundamental component of RNA is not yet fully understood. In our studies, we used a quadrupole time of flight (QTOF) capable of acquiring accurate mass data and the quadrupole ion trap (QIT) capable of providing sequential tandem MS data. Accurate mass of product-ions allows us to confirm their elemental composition while sequential dissociation of product-ions provides information about their structure. By combining these results with previously published data from isotopic labeling [16], ion spectroscopy [26], and theoretical [26–28] studies, we present a more detailed description of the reactivity of U during CID than existed previously. This work will be of interest to those studying the CID of nucleic acids and those

wishing to use tandem mass spectrometry for nontarget identification. Our integrated approach to describing charge-directed reaction mechanisms is widely applicable and could equally be applied to other classes of molecules of interest.

## Experimental

Ammonium acetate, uridine (99%), HPLC grade water, and methanol were purchased from Fisher Scientific (Nepean, ON, Canada). Uracil (≥99%) was purchased from Sigma Aldrich (Oakville, ON, Canada). Standard compounds were dissolved in a solution of 90:10 methanol:water with 0.1 mM ammonium acetate at an approximately 5 μM concentration.

The sequential dissociation study was carried out on a Thermo LCQ Deca ion trap mass spectrometer where standard was infused through the built in syringe pump at a rate of 5 μL/min. Spray voltage was 5 kV, capillary and tube lens offset voltages were both set to –10 V, and helium was used as a collision gas (Linde, Guelph, ON, Canada). For $MS^2$ and $MS^3$ experiments, the $q_z$ value was set to 0.25, and $MS^4$ experiments were carried out with $q_z$=0.35. For $MS^3$ and $MS^4$ experiments, the instrument's "low mass" setting was used along with automatic gain control. All collision energy (CE) values are presented in figure captions. In order to carry out the dissociation of protonated uracil at *m/z* 113, protonated uridine (*m/z* 245), which is known to produce abundant protonated uracil as its primary $MS^2$ dissociation product [12, 16], was infused and selected in $MS^2$. Protonated uracil at *m/z* 113 was then selected as the $MS^3$ precursor and its dissociation product selected as precursors in $MS^4$.

Accurate mass of product-ions was acquired using a QTOF Micro quadrupole time of flight mass spectrometer (Waters, Milford, MA) equipped with a nano-spray ESI ion source (Micromass, Manchester, UK). A Selectra (Ionalytics Corp., Ottawa, ON, Canada) high field asymmetric waveform ion mobility spectrometer (FAIMS), which was recently shown to separate protonated nucleosides and NA bases [1], was used with conditions identical to this previous report to separate protonated uridine from a background ion detected at *m/z* 113. By this method, an abundant source fragment corresponding to pure protonated uracil at *m/z* 113 could be continuously transmitted to the MS detector for single stage quadrupole dissociation in $MS^2$. Injections were made into a 400 nL/min flow of 0.1 mM ammonium acetate using the pump and autosampler of a nanoAcquity nano-flow LC system (Waters). Ionization was carried out in positive mode with a capillary voltage of 4500 V, a cone voltage of 25 V, and an extraction cone voltage of 1 V and Argon (Linde) was used as the collision gas. External mass calibration was carried out using glufibrinopeptide, and internal mass calibration was carried out using the known composition of the uracil precursor. This calibration gave a mass accuracy of 0.5 ppm in MS mode and of 1–35 ppm in MS/MS mode depending on *m/z* and abundance. These represent realistic mass accuracies for this instrument and were sufficient to establish elemental composition of all product-ions detected.

## Results and Discussion

Our first attempt to analyze a uracil standard by quadrupole time of flight (QTOF) and the quadrupole ion trap (QIT) showed a number of CID product-ions that had not been previously reported for uracil [16]. This was the result of an interfering isobaric *m/z* 113 ion contaminant present in the analyzed samples. To overcome this, we chose to use uridine (UR), which produces protonated U by elimination of a ribose moiety [12, 16]. For QIT, we were able to simply select $[UR + H]^+$ at *m/z* 245 in $MS^2$ in order to obtain $[U + H]^+$ at *m/z* 113 as a precursor in $MS^3$. The product-ion spectrum in $MS^3$ of protonated uracil by QIT-MS is shown in Figure 1A and shows abundant products of the loss of ammonia (–17), water (–18) and isocyanic acid (–HNCO, –43) as well as an ion-neutral reaction with residual water (+18) present as an impurity in the collision gas of our QIT [29].

For a QTOF, which is only capable of single stage MS/MS, source fragmentation was used to produce an abundant $[U + H]^+$ ion at *m/z* 113.0346. However, the isobaric background ion, which could be resolved at *m/z* 113.0952 in MS mode by the TOF detector was still selected for

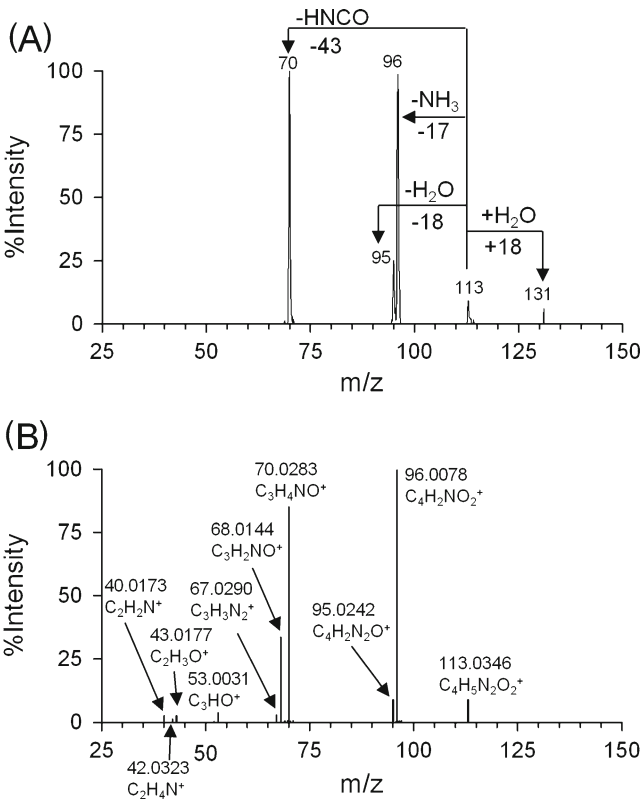


**Figure 1.** Product-ion spectra of protonated uracil at *m/z* 113 obtained by quadrupole ion trap MS at normalized collision energy=32 V (**A**) and the product-ion spectrum of protonated uracil obtained by quadrupole-time-of-flight MS at collision energy=24 V (**B**)

dissociation by the quadrupole mass analyzer. To separate these ions, we implemented high field asymmetric waveform ion mobility spectrometry (FAIMS), which operates as an ion filtering device between our ESI source and QTOF detector [1, 30]. We recently showed this technique to be capable of separating modified nucleosides and NA bases for MS/MS analysis even in the complex biological matrix of a urine sample [1] For our standard solution, FAIMS was easily able to separate $[UR + H]^+$ from the *m/z* 113 background ions before UR was fragmented in the source to form protonated U. In this way, we were able to deliver a continuous flow of pure protonated uracil for dissociation in the quadrupole of the QTOF and obtain the product-ion spectrum in Figure 1B.

This spectrum is comparable to previously published spectra with the absence of a few low abundance ions previously reported using different instrumentation [16]. The results of our accurate mass measurements annotated in Figure 1B agree with previously published data from isotope labeling studies carried out on U [16]. We have reinterpreted this labeling data, which was originally only discussed in terms of $^{15}N$, $^{13}C$, and $^{18}O$ labeling [16], to include the results from dissociation of [5,6-$D_2$]uracil that had not previously been explained but are critical in explaining several dissociation pathways. Based on this interpretation, the composition and atom position of each product-ion and all neutral losses are presented in Table 1, which is the starting point for our spectral interpretation.

## *Ionization, Tautomerization, and Collisional Activation of Uracil*

In solution, uracil is predominantly found in its diketo form shown in Scheme 1 and the most basic site on uracil, and hence the most likely to be protonated under electrospray conditions, is the keto oxygen $O^4$ [16, 28]. Once in the gas phase, ground state proton affinities of $O^2$ and $O^4$ become much closer in energy than in solution, and tautomerization and proton transfer are much more feasible [16].

We recently showed the importance of tautomeric form for the CID dissociation of a modified nucleoside [18]. This work also demonstrated that different reaction pathways of a nucleoside proceed exclusively from different tautomers that are formed during collisional activation [18]. Heterocyclic and highly conjugated uracil can be represented by eight different tautomeric forms, each with four different protonation sites for a total of at least 32 possible precursors to dissociation. The relative energies of all stable uracil tautomers and protonation sites were determined theoretically, revealing the N-1 protonated di-enol tautomer (I, all in Scheme 1) to be the lowest energy with the $O^4$ enol form II only slightly more energetic (~5 kJ $mol^{-1}$) [26–28]. Energy barriers for inter-conversion from I to the other stable tautomers range from 5 to 221 kJ $mol^{-1}$ [28]. Thus, regardless of the tautomeric form and protonation site of the original solution species, once protonated, the gas-phase ion is free to undergo proton transfer and tautomerization reactions as it is excited collisionally. Spectroscopic study of protonated uracil during infrared multiphoton dissociation (IRMPD) has confirmed the fact that multiple tautomers of protonated uracil are present in ion trap at energies associated with dissociation [26]. These results show at least two tautomers present at a threshold energy where the first fragment ions begin to appear.

It is reasonable to assume that at higher excitation energies, more energetic tautomers as well as their ring-opened products would be easily accessible, and that any of the 18 stable tautomers reported [28] can represent a viable precursor in CID. During excitation, some of these tautomers will adopt conformations from which simple charge-directed mechanisms can lead to dissociation upon further excitation. Scheme 1 shows those four stable tautomers (III–VI) that can account for all detected product ions of protonated uracil.

**Table 1.** Interpretation of Data from the CID of Stable Isotope Labeled Uracil in Nelson and McCloskey, 1994 [16]

| *m/z* | Product-ion[a] | Atoms lost[b] | Relative abundance of product-ion (%)[b] |
|---|---|---|---|
| 96 | $[M + H - NH_3]^+$ | N-1, $H^{5/6}$, $H_2^x$ | 10 |
| | | N-3, $H_3^x$ | 60 |
| | | N-3, $H^{5/6}$, $H_2^x$ | 30 |
| 95 | $[M + H - H_2O]^+$ | $O^2$, $H_2^x$ | 50 |
| | | $O^4$, $H_2^x$ | 50 |
| 70 | $[M + H - HNCO]^+$ | N-1, C-2, $O^2$, $H^x$ | 10 |
| | | N-3, C-2, $O^2$, $H^x$ | 50 |
| | | N-3, C-2, $O^2$, $H^{5/6}$ | 40 |
| 68 | $[M + H - NH_3\text{-}CO]^+$ | N-3, C-4, $O^4$, $H_3^x$ | 90 |
| | | N-3, C-2, $O^2$, $H_3^x$ | 10 |
| 67 | $[M + H - H_2O\text{-}CO]^+$ | C-2, $O^2$, $O^4$, $H_2^x$ | 100 |
| 53 | $[M + H - NH_3 - HNCO]^+$ and $[M + H - HNCO - NH_3]^+$ | N-1, C-2, $O^2$, N-3, $H^{5/6}$, $H_3^x$ | 100 |
| 43 | $[M + H - HNCO - HCN]^+$ | N-1, C-2, $O^2$, N-3, C-6, $H^{5/6}$, $H^x$ | 100 |
| 42 | $[M + H - HNCO - CO]^+$ | C-2, $O^2$, N-3, C-4, $O^4$, $H^x$ | 100 |
| 40 | $[M + H - NH_3 - CO - HCN]^+$ | C-2, $O^2$, N-3, C-4, $O^4$,$H^{5/6}$, $H_4^x$ | 100 |

[a]Product-ion origin determined from sequential ion trap dissociation.
[b]Determined from published data for CID of stable isotope labeled derivatives of uracil [16]. $H_n^x$ refers to the number of exchangeable protons lost, whose ring position cannot be specifically assigned by isotope labeling.

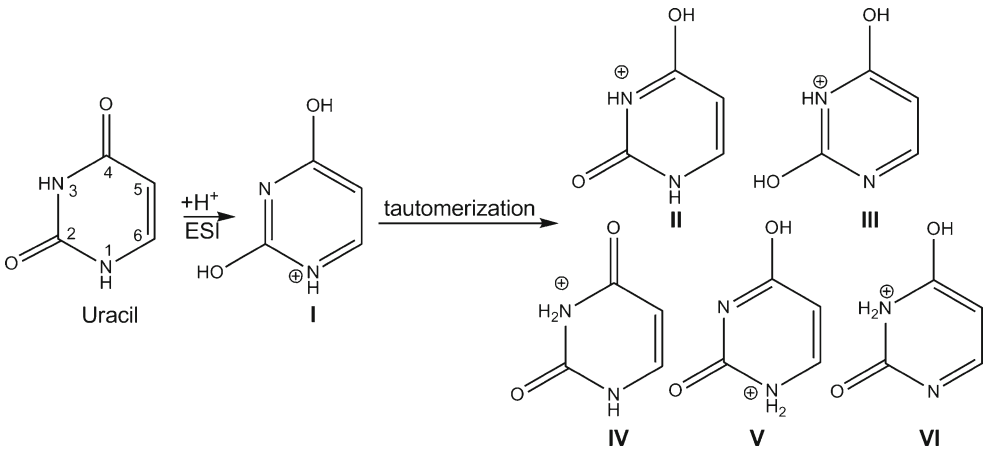


Scheme **1.**

For small, highly conjugated ions such as uracil, the charge site mediates all reaction steps, including proton transfer, charge redistribution, tautomerization, and ultimately dissociation [24]. Charge-directed dissociations proceed through favorable (stabilized) transition states to produce stable neutral molecules and product-ions. While compounds less readily able to interconvert between multiple tautomeric forms might dissociate through a single dissociation pathway, the multiple tautomers adopted by U in CID result in multiple dissociation pathways depending on the conformation of precursor ion during excitation. This is an important factor in describing CID reactivity that is often overlooked. The ion structures presented in Scheme 1 are the stable precursors of uracil that dissociate to form the detected product-ions when excited. For simplicity and space considerations, the dissociation mechanisms proposed in subsequent sections of this work begin from these precursors and do not show each step in tautomerization from the ground state ion I.

These tautomers provide the critical link between the complex dissociation pathways observed for uracil and a simple theory that can describe dissociation via charge-directed mechanisms [24] to form products with a stabilized charge [25]. By taking tautomerization into account, we can now explain all observed experimental data from an extensive isotopic labeling study, accurate mass measurements, and sequential tandem MS. The proposed reaction mechanisms are intended to show intramolecular interactions and stabilization of charge at critical points during dissociation. The proposed structures might not represent their lowest energy conformers, which could be calculated theoretically, but rather demonstrate the potential for charge stabilization at the transition state and in the product-ion, important factors in determining which dissociation processes are rational.

## *Ammonia Elimination from Protonated Uracil*

The primary dissociation product of uracil in Figure 1 is the product of ammonia loss detected at *m/z* 96. The results of isotope labeling (Table 1) show that at least three separate processes are occurring that result in elimination of ammonia. Based on all available data, three charge-directed processes for the elimination of ammonia from $[U + H]^+$ are proposed in Scheme 2. Contrary to previous interpretation of ammonia loss from pyrimidine rings [15, 16], Scheme 2 accounts for ammonia loss from N-3 with either exchangeable (Scheme 2A) or carbon bound (Scheme 2B) protons lost as well as ammonia loss form N-1 (Scheme 2C). For tautomer IV, ring opening at the C2–N3 bond (Scheme 2A) and proton transfer through a favorable six-membered ring conformation yield a quaternary ammonium precursor with charge localized at N-3. During dissociation of this transient species, charge developing at C-4 is stabilized by electron density from the conjugated system of double bonds and non-bonding electrons. The product of this reaction that represents, from Table 1, about 60% of the total signal detected at *m/z* 96, is also highly resonance stabilized and could be represented by six resonance structures (not shown). The final structure shown in Scheme 2A represents an overlay of these resonance structures with dashed bonds representing some contribution of π electron density. The same approach is used throughout the manuscript to show the potential for resonance stabilization of the charge.

A high degree of resonance stabilization can be shown for all abundant product-ions of uracil, demonstrating the importance of this factor in determining which product-ions are detected.

Ring opening of tautomer VI at the N3–C4 bond would induce a similar mechanism (Scheme 2B), where proton transfer would occur from C-5 that can account for 30% of the intensity of *m/z* 96 ion based on isotope labeling data (Table 1). Elimination of ammonia containing a C-5 bound proton could also occur after ring opening of tautomer V at the N-1/C-2 position (Scheme 2C). This reaction accounts for both the 10% of intensity of the *m/z* 96 product ion attributed to N-1 loss as well as the remaining 10% of ammonia loss including a C-bound proton (Table 1). The transfer of $H^5$ to form a quaternary ammonium ion before

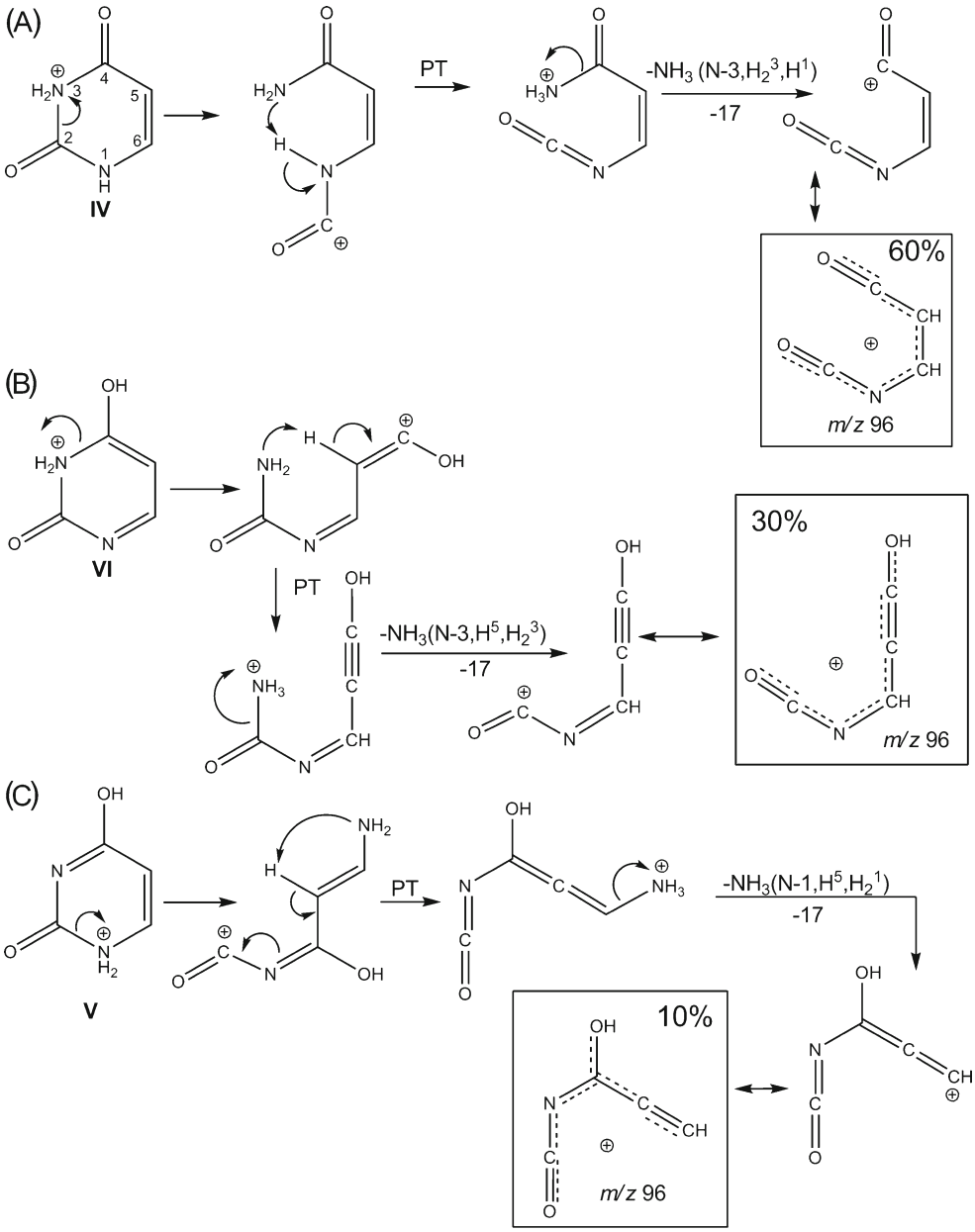


Scheme 2.

ammonia elimination differs significantly from proton scrambling prior to dissociation. This phenomenon, previously reported for the nucleobase guanine [18] and considered as a possible explanation for puzzling results for the CID of [5,6-$D_2$]Uracil [16], can be completely ruled out based on experimental data in the case of uracil.

Dissociation of the *m/z* 96 ion in $MS^4$ mode (Figure 2A) supports the structures proposed in Scheme 2. The *m/z* 96 ions dissociate by elimination of CO to produce an abundant ion with *m/z* 68, elimination of HNCO to produce an abundant ion with *m/z* 53, and elimination of ethyne (–HC ≡ CH) to produce a minor product ion with *m/z* 70. Based on labeling data (Table 1) and on the precursor ions proposed in Scheme 2 these second generation products have been assigned to a specific *m/z* 96 precursor in the pathways in Scheme 3.

## *Elimination of Water from Protonated Uracil*

Like ammonia loss, previous proposals for the mechanism of water loss from pyrimidine bases have involved ring opening followed by proton transfer to an exocyclic oxygen [15, 16].

This proposal does not fit experimental data. Isotope labeling data in Table 1 show a ratio of 1:1 for loss of water from $O^2$ and $O^4$, which is significant in that it suggests equivalent mechanisms for each process. Also important is the fact that neither of these processes shows proton transfer

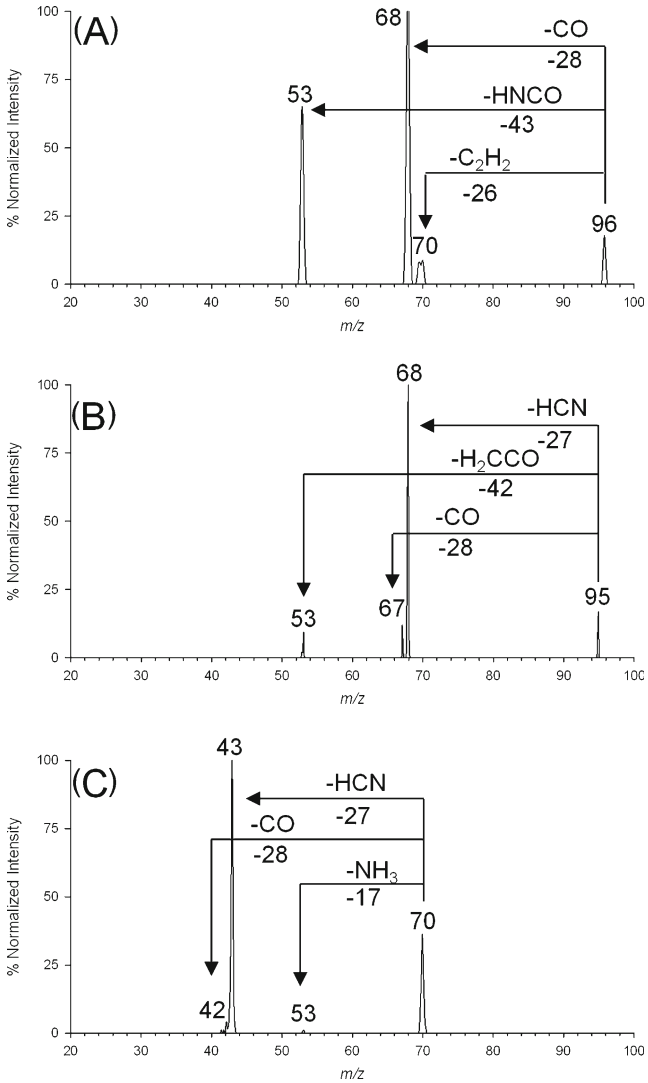


**Figure 2.** Sequential dissociation of major products of protonated uracil in $MS^4$ using QIT-MS. (**A**) CID of the *m/z* 96 products of ammonia loss at NCE=32 V. (**B**) CID of the *m/z* 95 product of water loss at NCE=29 V. (**C**) CID of the *m/z* 70 product of isocyanic acid loss at NCE=32 V

from C-5 or C-6 to O before water elimination as was the case for ammonia elimination in Scheme 2B and C. After ring opening at any position, $O^2$ and $O^4$ will not be equivalent with respect to proton transfer reactions and the rate of water loss. Furthermore, reasonable charge-directed mechanisms involving initial ring opening followed by water loss would involve proton transfer from C-5 or C-6, which does not occur. However, by taking into account all possible tautomers, it is evident that tautomer III (Scheme 1) is a reasonable precursor from which water can be lost without ring opening and where $O^2$ and $O^4$ are nearly equivalent.

Proposals that account for both the equivalent loss of $O^2$ and $O^4$ as well as product-ions of subsequent stages of sequential tandem mass spectrometry are presented in Scheme 4A and B. Water elimination from either of these precursors is favorable because of resonance stabilization of the developing charge at either C-4 or C-2. Further, stabilization of the charge on the product-ions is significant and nearly equivalent between the two structures.

Dissociation of the *m/z* 95 ion in $MS^4$ mode (Figure 2B) supports the structures proposed in Scheme 4. The *m/z* 95 ions dissociate by elimination of hydrogen cyanide (–HCN) to produce an abundant ion with *m/z* 68, elimination of CO to produce a product ion with *m/z* 67, and elimination of ketene ($–H_2CCO$) to produce a product ion with *m/z* 53. Based on labeling data (Table 1) and on the precursor ions proposed in Scheme 4, these second generation products have been assigned to a specific *m/z* 95 precursor in the pathways in Scheme 3.

## *Elimination of Isocyanic Acid from Protonated Uracil*

Based on the isotope labeling data in Table 1, at least three different mechanisms exist for elimination of isocyanic acid (–HNCO, –43) from protonated uracil during CID. The primary isomer of *m/z* 70 involves loss of $O^2$ and N-3 and retention of $O^4$ and N-1 with loss of either an exchangeable (N or O bound) proton or a C-5/C-6 bound proton at a ratio 5:4. The previously proposed retro-Deils-Alder (RDA) reaction [14–16] of the $O^4$ protonated di-keto tautomer shown in Scheme 5A is unsatisfactory for several reasons. This reaction cannot occur in a single step as a charge-directed process, but rather would need to first undergo tautomerization or else ring opening at C-2/N-1 before elimination of isocyanic acid could occur. Even if this were to occur, the ion shown in Scheme 5A does not represent a stable product and would never be detected. Charge is localized on the $O^4$ carbonyl group and not stabilized by the abundant π electron density in the rest of the ion. If formed, this ion would represent a reactive intermediate that could be expected to immediately eliminate ketene ($–H_2CCO$, –42) by the mechanism shown in Scheme 5B to form protonated hydrogen cyanide at *m/z* 28, which was not detected as a first generation product-ion of protonated uracil in Figure 1, but has been reported previously [16].

Scheme 5C shows a proposal for an alternative charge-directed process, also induced by proton transfer to $O^4$ in the N-3 protonated diketo tautomer IV that would lead to the abundant elimination of HNCO from $O^2$, C-2, and N-3. Instead of the RDA reaction previously proposed [16], an intramolecular nucleophilic attack by N-1 at C-4 creates an activated precursor from which isocyanic acid can be eliminated to produce an *m/z* 70 product-ion with charge delocalized throughout the ion. According to Table 1, approximately 50% of the detected abundance at *m/z* 70 originates from dissociation through this pathway, without loss of $H^5$ or $H^6$.

About 40% of the *m/z* 70 product-ion in Figure 1 originates from a pathway that does involve loss of a proton from C-5 or C-6 and its loss during dissociation. This reaction can be rationalized through a similar mechanism to

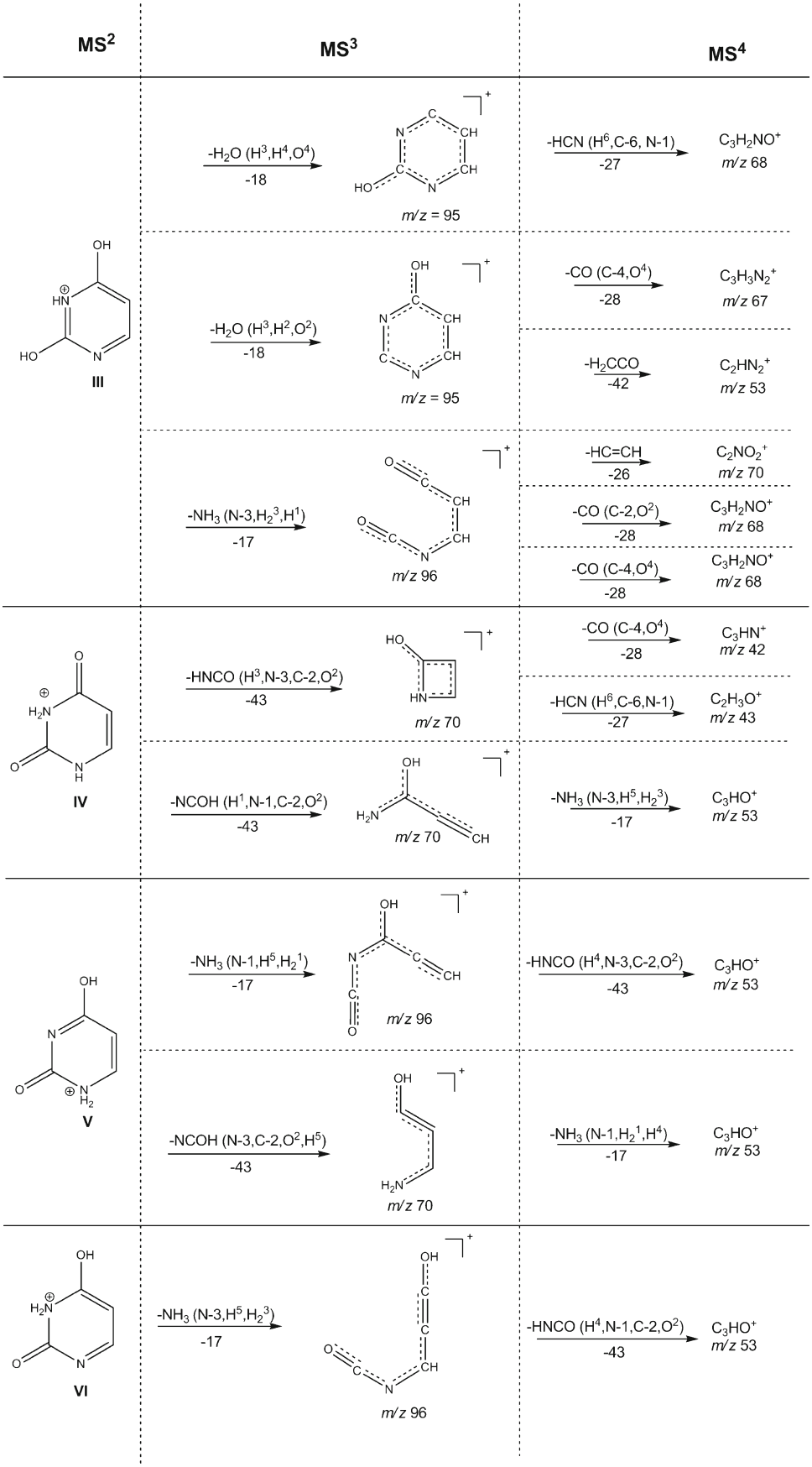
MS2
MS3
MS4
III
IV
V
VI
-H2O (H3,H4,O4)
-18
m/z = 95
-HCN (H6,C-6, N-1)
-27
C3H2NO+
m/z 68
-H2O (H3,H2,O2)
-18
m/z = 95
-CO (C-4,O4)
-28
C3H3N2+
m/z 67
-H2CCO
-42
C2HN2+
m/z 53
-NH3 (N-3,H2 3,H1)
-17
m/z 96
-HC=CH
-26
C2NO2+
m/z 70
-CO (C-2,O2)
-28
C3H2NO+
m/z 68
-CO (C-4,O4)
-28
C3H2NO+
m/z 68
-HNCO (H3,N-3,C-2,O2)
-43
m/z 70
-CO (C-4,O4)
-28
C3HN+
m/z 42
-HCN (H6,C-6,N-1)
-27
C2H3O+
m/z 43
-NCOH (H1,N-1,C-2,O2)
-43
m/z 70
-NH3 (N-3,H5,H2 3)
-17
C3HO+
m/z 53
-NH3 (N-1,H5,H2 1)
-17
m/z 96
-HNCO (H4,N-3,C-2,O2)
-43
C3HO+
m/z 53
-NCOH (N-3,C-2,O2,H5)
-43
m/z 70
-NH3 (N-1,H2 1,H4)
-17
C3HO+
m/z 53
-NH3 (N-3,H5,H2 3)
-17
m/z 96
-HNCO (H4,N-1,C-2,O2)
-43
C3HO+
m/z 53

Scheme 3.

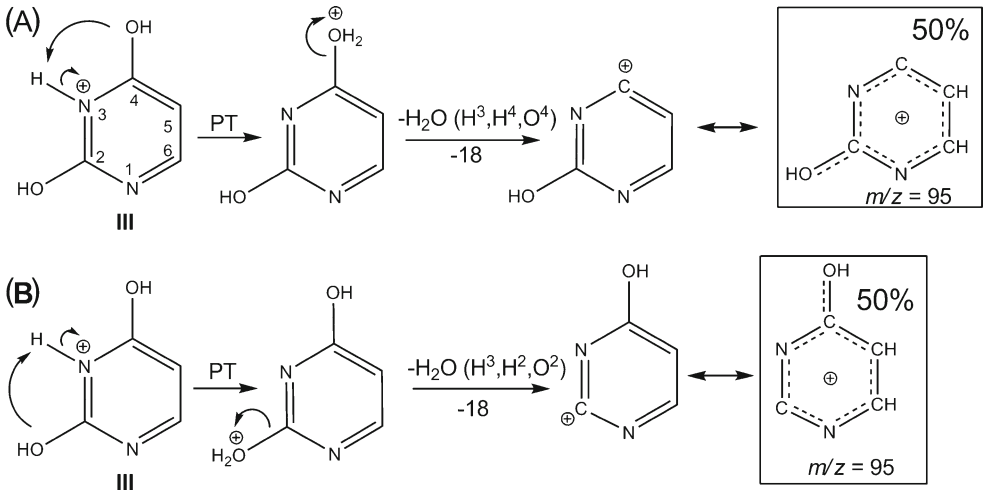


Scheme 4.

those leading to ammonia loss in Scheme 2 with abstraction of a proton from C-5. In Scheme 5D, after ring opening of the $O^4$ enol tautomer V at N-1/C-2, an intermediate identical to that shown in Scheme 2C as a precursor to ammonia loss is formed. If the C-5 proton is abstracted by $O^4$ as shown in Scheme 5D or N-3 (not shown) as opposed to N-1, charge

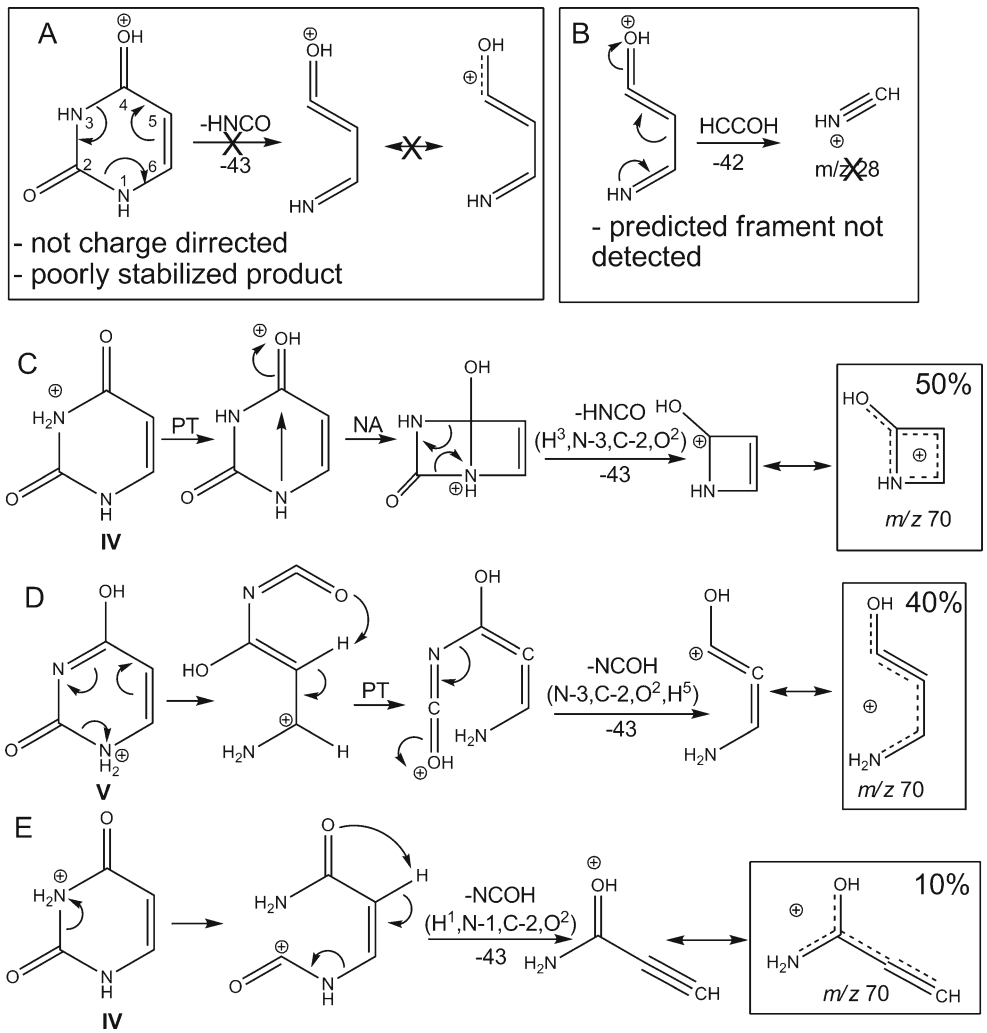


Scheme 5.

becomes localized on the other side of the molecule leading to elimination of cyanic acid (NCOH) or isocyanic acid (not shown), respectively. Table 1 also shows that minor contributions to *m/z* 70 from loss of HNCO from N-3/C-4/$O^4$ could occur by abstraction of H-5 by $O^2$ after ring opening at C-2/N-3 as shown in Scheme 5E.

Dissociation of the *m/z* 70 ion in $MS^4$ mode (Figure 2C) supports the structures proposed in Scheme 5. The *m/z* 70 ions dissociate by elimination of ketene to produce an abundant ion with *m/z* 43, elimination of ammonia to form a product ion with *m/z* 53, and elimination of CO to produce a minor product ion with *m/z* 42. Based on labeling data (Table 1) and on the precursor ions proposed in Scheme 5, these second generation products have been assigned to a specific *m/z* 70 precursor in the pathways in Scheme 3.

## Conclusion

By combining our accurate mass and sequential tandem MS results with previously published data from isotope labeling, theoretical, and ion-spectroscopy studies, we have been able to describe the reactivity of uracil during CID in much greater detail than was previously possible. We show that the very complex reactivity of this heterocyclic ion is the result of its propensity to undergo tautomerization in the gas-phase before dissociation so that multiple precursor ions are present for a single species. This leads to numerous dissociation pathways possible for each observed neutral loss.

All reactions proposed for protonated uracil also have important implications for the tandem mass spectrometry identification of modified forms of uracil in biological samples. As a result of chemical modification of uracil, reactions established for the unmodified base can be suppressed or enhanced or new reaction can be induced. This valuable information can be used for structural elucidation of derivatives of uracil now that mechanisms of its fundamental reactions are better understood.

In total we have examined 20 reactions in the current work as well as the hundreds of others in our previous published [1, 4–7, 18] and unpublished studies. Based on these reactions, we are able to make some generalizations about what makes a mechanistic proposal suitable for describing the dissociation of small even electron ions during CID. In general: (1) All reaction steps can be described as charge-directed processes. (2) Collisionally excited ions can adopt higher energy conformations that are the precursors to dissociation. (3) The activated precursor offers stabilization to the charge developing during the dissociation step. (4) The product of dissociation is stabilized by delocalization of the charge as much as possible given the structure and formula of the ion. (5) Ions with a localized charge are transient species prone to rapid fragmentation and are generally not detected in MS/MS spectra. (6) Any bond making (nucleophilic attack) or non-dissociative bond breaking (ring opening) occurs prior to elimination of a neutral, which is the final step of reaction forming a stable product.

By using these simple generalizations as a starting point for describing reactivity, spectral differences observed between related species can usually be described and understood based on real chemical principles such as steric or electronic effects. The conformations generated from these mechanisms can serve as a reasonable starting point for more detailed theoretical studies of CID reaction mechanism. Further, this type of an understanding of reactivity can be used to develop structural proposals for unknown molecules during nontarget analysis based on the known reactivity of compounds with structural similarities.

## Acknowledgments

The authors thank the National Sciences and Engineering Council of Canada (NSERC), the Ontario Ministry of Training, Colleges and Universities, and the Canadian Foundation for Innovation (CFI) for their financial support.

## References

1. Beach, D.G., Gabryelski, W.: Nontarget Analysis of Urine by Electrospray Ionization-High Field Asymmetric Waveform Ion Mobility-Tandem Mass Spectrometry (ESI-FAIMS-MS/MS). *Anal. Chem.* **83**, 9107–9133 (2011)
2. Gates, K.S.: An Overview of Chemical Processes That Damage Cellular DNA: Spontaneous Hydrolysis, Alkylation, and Reactions with Radicals. *Chem. Res. Toxicol.* **22**, 1747–1760 (2009)
3. Wurtmann, E.J., Wolin, S.L.: RNA Under Attack: Cellular Handling of RNA Damage. *Crit. Rev. Biochem. Mol. Biol.* **44**, 34–49 (2009)
4. Sultan, J., Gabryelski, W.: Structural Identification of Highly Polar Nontarget Contaminants in Drinking Water by ESI-FAIMS-Q-TOF-MS. *Anal. Chem.* **78**, 2905–2917 (2006)
5. Gabryelski, W., Frose, K.L.: Characterization of Naphthenic Acids by Electrospray Ionization High-Field Asymmetric Waveform Ion Mobility Spectrometry Mass Spectrometry. *Anal. Chem.* **75**, 4612–4623 (2003)
6. Kulikova, N., Baker, M., Gabryelski, W.: Collision Induced Dissociation of Protonated *N*-Nitrosodimethylamine by Ion Trap Mass Spectrometry: Ultimate Carcinogens in Gas Phase. *Int. J. Mass. Spectrom* **288**, 75–83 (2009)
7. Baker, M., Gabryelski, W.: Collision Induced Dissociation of Deprotonated Glycolic Acid. *Int. J. Mass Spectrom.* **262**, 128–135 (2007)
8. Harvey, D.J.A.: New Charge-Associated Mechanism to Account for the Production of Fragment Ions in the High-Energy CID Spectra of Fatty Acids. *J. Am. Soc. Mass Spectrom.* **16**, 280–290 (2005)
9. Lewis-Stanislaus, A.E., Li, L.: A Method for Comprehensive Analysis of Urinary Acylglycines by Using Ultra-Performance Liquid Chromatography Quadrupole Linear Ion Trap Mass Spectrometry. *J. Am. Soc. Mass Spectrom.* **21**, 2105–2116 (2010)
10. Weissberg, A., Dagan, S.: Interpretation of ESI(+)-MS-MS spectra-Towards the Identification of "Unknowns. *Int. J. Mass Spectrom.* **299**, 158–168 (2011)
11. Rache, F., Svatos, A., Madula, R.K., Bottches, C., Bocker, S.: Computing Fragmentation Trees from Mass Spectrometry Data. *Anal. Chem.* **83**, 1243–1251 (2011)
12. Horia, H., Arita, M., Kanaya, S., Nihei, Y., Ikeda, T., Suwa, K., Ojima, Y., Tanaka, K., Tanaka, S., Soshima, K., Oda, Y., Kakazu, Y., Kusano, M., Tohge, T., Matsuda, F., Sawada, Y., Hirai, M.Y., Nakanishi, H., Ikeda, K., Akimoto, N., Maoka, T., Takahashi, H., Ara, T., Sakurai, N., Suzuki, H., Shibata, D., Nuemann, S., Iida, T., Tanaka, K., Funatsu, K., Matsuura, F., Soga, T., Taguchi, R., Saito, K., Nishioka, T.: MassBank: A Public Repository for Sharing Mass Spectral Data for Life Sciences. *J. Mass Spectrom.* **45**, 703–714 (2010)
13. Wishart, D.S., Knox, C., Guo, A.C., Eisner, R., Young, N., Gautam, B., Hau, D.D., Psychogios, N., Dong, E., Bouatra, S., Mandal, R., Sinelnikov, I., Xia, J., Jia, L., Cruz, J.A., Lim, E., Sobsey, C.A., Shrivastava, S., Huang, P., Liu, P., Fang, L., Peng, J., Fradette, R.,

Cheng, D., Tzur, D., Clements, M., Lewis, A., De Souza, A., Zuniga, A., Dawe, M., Xiong, Y., Clive, D., Greiner, R., Nazyrova, A., Shaykhutdinov, R., Li, L., Vogel, H.J.: HMDB: A Knowledgebase for the Human Metabolome. *Nucleic Acids Res.* **37**, D603–D610 (2009)
14. Gregson, J.M., McCloskey, J.A.: Collision-Induced Dissociation of Protonated Guanine. *Int. J. Mass Spectrom. Ion Process* **165/166**, 475–485 (1997)
15. Jensen, S.S., Ariza, X., Nielsen, P., Vilarrasa, J., Kirpekar, F.: Collision-Induced Dissociation of Cytidine and Its Derivatives. *J. Mass Spectrom.* **42**, 49–57 (2007)
16. Nelson, C.C., McCloskey, J.A.: Collision-Induced Dissociation of Uracil and Its Derivatives. *J. Am. Soc. Mass Spectrom.* **5**, 339–349 (1994)
17. Nelson, C.C., McCloskey, J.A.: Collision-Induced Dissociation of Adenine. *J. Am. Chem. Soc.* **114**, 3661–3668 (1992)
18. Sagoo, S., Beach, D.G., Manderville, R.A., Gabryelski, W.: Tautomerization in Gas Phase Ion Chemistry of Isomeric C-8 Deoxyguanosine Adducts From Phenol-Induced DNA Damage. *J. Mass Spectrom.* **46**, 41–49 (2011)
19. Kammere, B., Frickenschmidt, A., Muller, C.E., Laufer, S., Gleiter, C. H., Liebich, H.: Mass Spectrometric Identification of Modified Urinary Nucleosides Used as Potential Biomedical Markers by LC-ITMS Coupling. *Anal. Bioanal. Chem.* **382**, 1017–1026 (2005)
20. Bullinger, D., Fux, R., Nicholson, G., Plontke, S., Belka, C., Laufer, S., Gleiter, C.H., Kammerer, B.: Identification of Urinary Modified Nucleosides and Ribosylated Metabolites in Humans Via Combined ESI-FTICR MS and ESI-IT-MS Analysis. *J. Am. Soc. Mass Spectrom.* **19**, 1500–1513 (2008)
21. Li, H., Wang, S., Liu, H., Bu, S., Li, J., Han, D., Zhang, M., Wu, G.: Separation and Identification of Purine Nucleosides in the Urine of Patients with Malignant Cancer by Reverse Phase Liquid Chromatography/Electrospray Tandem Mass Spectrometry. *J. Mass Spectrom.* **44**, 641–651 (2009)
22. Hua, Y., Wainhaus, S.B., Yang, Y., Lixing, S., Xiong, Y., Xu, X., Zhang, F., Bolton, J., van Breemen, R.B.: Comparison of Negative and Positive Ion Electrospray Tandem Mass Spectrometry for the Liquid Chromatography Tandem Mass Spectrometry Analysis of Oxidized Deoxynucleosides. *J. Am. Soc. Mass Spectrom.* **12**, 80–87 (2000)
23. Cheng, C., Gross, M.L.: Applications and Mechanisms of Charge-Remote Fragmentation. *Mass Spectrom. Rev.* **19**, 398–420 (2000)
24. Afonso, C., Cole, R.B., Tabet, J.: Dissociation of Even-Electron Ions. In: Cole, R.B. (ed.) Electrospray and MALDI Mass Spectrometry, p. 631. Wiley, Hoboken, NJ (2010)
25. McLafferty, F.W.: Interpretation of Mass Spectra, 2nd edn, p. 45. WA Benjamin Inc, Reading, MA (1973)
26. Salpin, J., Guillaumont, S., Tortajada, J., MacAleese, L., Lemaile, J., Maitre, P.: Infrared Spectra of Protonated Uracil, Thymine, and Cytosine. *Chem. Phys. Chem.* **8**, 2235–2244 (2007)
27. Kryachko, E.S., Nguyen, M.T., Zeegers-Huyskens, T.: Theoretical Study of Tautomeric Forms of Uracil. 1. Relative Order of Stabilities and Their Relation to Proton Affinities and Deprotonation Enthalpies. *J. Phys. Chem. A* **105**, 1288–1295 (2001)
28. Wolken, J.K., Turecek, F.: Proton Affinity of Uracil. A Computational Study of Protonation Sites. *J. Am. Soc. Mass Spectrom.* **11**, 1065–1071 (2000)
29. Tuytte, R., Lemier, F., Esmans, E.L., Herrebout, W.A., van der Veken, B.J., Dudley, E., Newton, R.P., Witters, E.: In-Source CID of Guanosine: Gas Phase Ion–Molecule Reactions. *J. Am. Soc. Mass Spectrom.* **17**, 1050–1062 (2006)
30. Klakowski, B.M., Mester, Z.: Review of Applications of High-Field Asymmetric Waveform Ion Mobility Spectrometry (FAIMS) and Differential Mobility Spectrometry (DMS). *Analyst* **132**, 842–864 (2007)